THE JOURNAL OF PHYSICAL CHEMISTRY B

Article

pubs.acs.org/JPCB

Hydroxyl Radical Reaction with *trans*-Resveratrol: Initial Carbon Radical Adduct Formation Followed by Rearrangement to Phenoxyl Radical

Dan-Dan Li,[†] Rui-Min Han,*[,†] Ran Liang,[†] Chang-Hui Chen,[†] Wenzhen Lai,[†] Jian-Ping Zhang,[†] and Leif H. Skibsted*[,‡]

[†]Department of Chemistry, Renmin University of China, Beijing 100872, P. R. China

[‡]Food Chemistry, Department of Food Science, University of Copenhagen, Rolighedsvej 30, DK-1958 Frederiksberg C, Denmark

Supporting Information

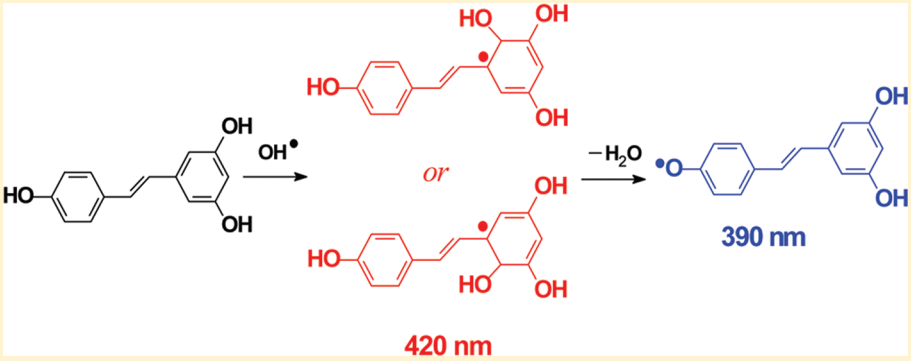

ABSTRACT: In the reaction between *trans*-resveratrol (resveratrol) and the hydroxyl radical, kinetic product control leads to a short-lived hydroxyl radical adduct with an absorption maximum at 420 nm and a lifetime of 0.21 ± 0.01 μs (anaerobic acetonitrile at 25 °C) as shown by laser flash photolysis using *N*-hydroxypyridine-2(1*H*)-thione (N-HPT) as a "photo-Fenton" reagent. The transient spectra of the radical adduct are in agreement with density functional theory (DFT) calculations showing an absorption maximum at 442 or 422 nm for C2 and C6 hydroxyl adducts, respectively, and showing the lowest energy for the transition state leading to the C2 adduct compared to other radical products. From this initial product, the relative long-lived 4′-phenoxyl radical of resveratrol (τ = 9.9 ± 0.9 μs) with an absorption maximum at 390 nm is formed in a process with a time constant (τ = 0.21 ± 0.01 μs) similar to the decay constant for the C2 hydroxyl adduct (or a C2/C6 hydroxyl adduct mixture) and in agreement with thermodynamics identifying this product as the most stable resveratrol radical. The hydroxyl radical adduct to phenoxyl radical conversion with concomitant water dissociation has a rate constant of 5×10^6 s^{-1} and may occur by intramolecular hydrogen atom transfer or by stepwise proton-assisted electron transfer. Photolysis of N-HPT also leads to a thiyl radical which adds to resveratrol in a parallel reaction forming a sulfur radical adduct with a lifetime of 0.28 ± 0.04 μs and an absorption maximum at 483 nm.

1. INTRODUCTION

trans-Resveratrol (*trans*-3,5,4′-trihydroxystilbene, RES, Scheme 1) is a plant phytoalexin abundant in grapes, peanuts, and mulberries, and one of the plant phenols getting increasing attention as a food factor important for human health. Resveratrol has been associated with interesting biomedical properties such as inhibitory effects on cancer promotion and propagation, and has been suggested to yield protection against cardiovascular diseases due to its distinct antioxidant activities.[1−5] The antioxidant activity of resveratrol is related to the ability of inhibiting lipid and protein peroxidation through scavenging of reactive oxygen species (ROS) such as $LOO^•$, $HOO^•$, $^•OH$, and $O_2^{•-}$, which all are involved in the pathophysiology of aging and a multitude of lifestyle-related diseases such as cancer, Alzheimer's disease, Parkinson's disease, and various cardiovascular diseases.[6−8]

It is well established that resveratrol scavenges free radicals efficiently due to the resonance stabilized structures of the phenoxyl radicals resulting from scavenging of oxidizing

Scheme 1. Molecular Structure of Resveratrol

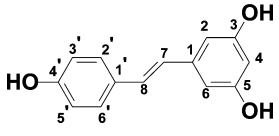

Received: April 7, 2012
Revised: May 23, 2012
Published: May 31, 2012

radicals.[9] As demonstrated in many experimental studies on the radical scavenging reactions of resveratrol, the 4′-hydroxyl group is the most reducing and has the highest acidity among the three phenolic groups of resveratrol.[10,11] The kinetics and mechanism of resveratrol reaction with ROS are, however, only sparsely studied and, for resveratrol, it is not even established whether radical scavenging occurs through hydrogen atom transfer (HAT), electron transfer (ET), or radical adduct formation (RAF). Especially, the mechanism of resveratrol reaction with •OH, as the most reactive oxygen species with its short half-lifetime of 10^{-9} s, is still controversial, and systematic investigations are lacking.[12]

In the present study, we have accordingly investigated the kinetics of the reaction of resveratrol with •OH generated from the "photo-Fenton" reagent *N*-hydroxypyridine-2(1*H*)-thione (N-HPT) in acetonitrile using time-resolved spectroscopy. The reaction of resveratrol with the PyS• thiyl radical, concomitantly formed with the hydroxyl radical through homolytical cleavage of N-HPT, was also investigated. The role of sulfur radicals in redox regulation in biological systems is increasingly in focus, especially in relation to protein modification and function, and the study of the reaction of resveratrol with thiyl radical is also highly relevant in this context.[13]

2. MATERIALS AND METHODS

Sample Preparation. *N*-Hydroxypyridine-2(1*H*)-thione (N-HPT, >99%, Alfa Aesar, Tianjin, China) was recrystallized twice before use in a binary solvent of ethanol/water = 1:1 (v/v). HPLC-grade acetonitrile (Fisher Scientific, Fair Lawn, NJ) was used as received. *trans*-Resveratrol (resveratrol, RES, 98%) was purchased from Huike Plant Exploitation Inc., Shanxi, China. Methyl methacrylate (MMA, 99%) and *tert*-butyl alcohol (*t*-BuOH, 99%) were purchased from Alfa Aesar Co., Ltd. (Tianjin, China).

Laser Flash Photolysis. The laser flash photolysis device has been described elsewhere.[14] The excitation laser pulses at 355 nm (3 mJ/pulse, 7 ns, 10 Hz) were supplied by Nd^{3+}:YAG laser (Quanta-Ray PRO-230, Spectra Physics, Inc., Mountain View, CA), and the probe light was provided by a xenon-flash lamp synchronized to the electric gate of the ICCD detector (L7685, Hamamatsu Photonics, Hamamatsu City, Japan). The optical path length of the flow cuvette (~50 mL) used for the laser flash photolysis was 1 mm, and 1 cm cell was used for steady-state absorption spectra determination. The anaerobic condition was achieved by bubbling the solution with high-purity argon. The concentration of N-HPT was 1.5×10^{-3} M, while the concentration of resveratrol was 1.0×10^{-2} M. The solution samples were used immediately after preparation. All of the measurements were carried out at room temperature (~25 °C).

Computational Details. For the reaction of resveratrol with •OH, three HAT and 14 RAF pathways were considered. The geometry optimizations were preformed in the gas phase with the hybrid meta-GGA M06-2X functional and 6-31G* basis set. Each stationary point was classified as a minimum or transition state by the frequency calculations. The absorption energies and intensities of the products in all the studied channels were calculated using the time-dependent density functional theory (TDDFT) method, and then were transformed with the Swizard program[15] into simulated spectra. The effect of solvent, acetonitrile, was included by using the integral-equation-formalism polarizable continuum model (IEF-PCM)[16] in the single-point calculations and TDDFT calculations at the M06-2X/6-31G* level. All calculations were carried out with the Gaussian 09 program package.[17]

3. RESULTS

Steady-State Absorption Spectroscopy. Figure 1 shows the steady-state absorption spectra of N-HPT (4.6×10^{-5} M) and resveratrol (RES, 3.7×10^{-6} M) in acetonitrile as determined using 1 cm optical cell. Arrow indicates the excitation wavelength λ_{exc} = 355 nm.

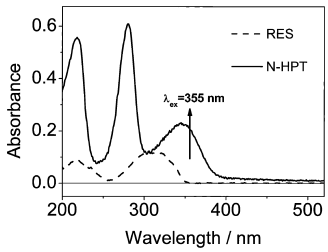

Figure 1. UV−visible absorption spectra of N-HPT (4.6×10^{-5} M) and resveratrol (RES, 3.7×10^{-6} M) in acetonitrile as determined using 1 cm optical cell. Arrow indicates the excitation wavelength λ_{exc} = 355 nm.

Laser Flash Photolysis. *Photochemistry of Resveratrol.* The transient absorption spectra and their time evolution following 355 nm laser photoexcitation of resveratrol (1.0×10^{-2} M) in acetonitrile are presented in Figure 2, a and b. A broad absorption band with a maximum at 500 nm completely decays on a 500 ns time scale with a time constant of $\tau = 0.08 \pm 0.02$ μs. This transient species was quenched by oxygen on change from anaerobic to aerobic conditions as seen in Figure S1 in the Supporting Information. This species is accordingly ascribed to a resveratrol triplet excited-state, ^{3}RES*.

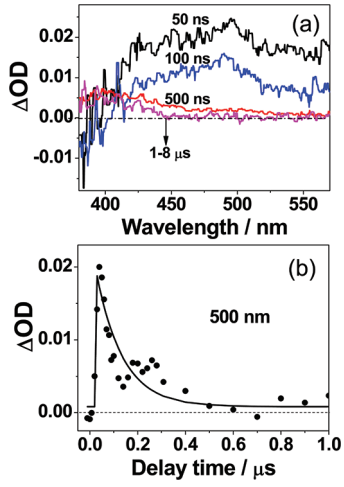

Figure 2. Transient absorption spectra (a) and corresponding time evolution profile at 500 nm (b) under anaerobic conditions of resveratrol (1.0×10^{-2} M) in acetonitrile following photoexcitation at 355 nm (3 mJ/pulse).

At longer delay time (longer than 1.0 μs), a long-lived species with a maximum at ~390 nm and with a broad and unstructured absorption decays with a slower rate. The transient spectra of this species are distinctly different from those of ^{3}RES*. It has been found in our previous investigations

dx.doi.org/10.1021/jp3033337 | J. Phys. Chem. B 2012, 116, 7154−7161

that ultraviolet laser excitation may induce the dissociation of phenolic O−H and produce the corresponding phenoxyl neutral radical. 4′-Hydroxyl of resveratrol is reported having lower bond dissociation energy and lower redox potential than the two 3- and 5-hydroxyls.[18,19] The stable radical species observed in this study at 1−8 μs is similar in spectral features to the 4′-phenoxyl radical generated from the reaction of resveratrol with the reactive $(CH_3)_3CO^{\bullet}$ by hydrogen atom transfer (HAT) and is thus assigned to the 4′-resveratrol radical formed from photodissociation of excited resveratrol.[18] The definite lifetime for the resveratrol 4′-phenoxyl radical was found difficult to determine due to the rather low absorption intensity of the 4′-phenoxyl radical.

Reaction of Resveratrol with Excited N-HPT. (1). Photochemistry of N-HPT. Photoexicitation of N-HPT homolytically cleaves the N−O bond and gives rise to the 2-pyridylthiylradical ($PyS^{\bullet}$) and the hydroxyl radical ($^{\bullet}OH$) as shown in the reaction of eq 1, which has been established in previous work.[14,20] Figure 3a shows the transient absorption spectra for

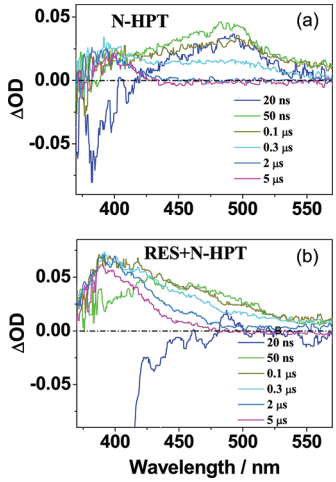

Figure 3. Transient absorption spectra of N-HPT (1.5×10^{-3} M) in the absence (a) and in the presence (b) of resveratrol (RES, 1.0×10^{-2} M) in acetonitrile following photoexcitation at 355 nm (3 mJ/pulse) under anaerobic condition.

N-HPT in acetonitrile following 355 nm photoexcitation. Briefly, the broad-band transient (400−550 nm, 20−300 ns), decaying out within 2.0 μs, is ascribed to the absorption superposition of $PyS^{\bullet}$ in large amount and a small quantity of the N-HPT triplet excited state ^{3}(N-HPT)*. The species absorbing with a maximum around 400 nm lasting for longer than 2.0 μs have been definitely confirmed to be the stable product PySSPy formed from the $PyS^{\bullet}$ dimerization.

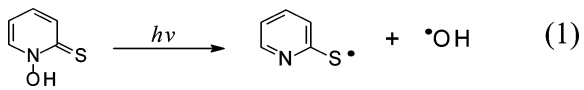

(2). Reaction of Resveratrol with Excited N-HPT. Transient absorption spectra of resveratrol (1.0×10^{-2} M) and N-HPT (1.5×10^{-3} M) in acetonitrile following 355 nm excitation under anaerobic condition are shown in Figure 3b. The sharp negative signal observed at initial delay time (20 ns) in Figure 3b arises from the fluorescence emission of the resveratrol singlet excited state ^{1}RES*, which is also observed at the same delay time for direct photoexcitation of resveratrol (*data not shown*). Compared with the signal in Figure 3a, it is obvious that the absorbance intensity of $PyS^{\bullet}$ at 400−550 nm at 50 ns as seen in Figure 2b notably is reduced in the presence of resveratrol, which indicates that $PyS^{\bullet}$ is being scavenged by resveratrol. On the other hand, the absorption intensity at 400 nm, which has been ascribed to the absorption of PySSPy product in Figure 3a, greatly increases and gets broader at longer wavelength, indicating that new products are formed from the reaction of resveratrol with reactive species generated from photoexcitation of N-HPT, such as $PyS^{\bullet}$, $^{\bullet}OH$ or ^{3}(N-HPT)*.

Time evolution profiles of relevance to the transient absorption spectra of N-HPT (1.5×10^{-3} M) and resveratrol (1.0×10^{-2} M), as shown in Figure 3b and probed at the indicated wavelengths in acetonitrile following photoexcitation, are shown in Figure 4. It is clearly seen in Figure 4 that the

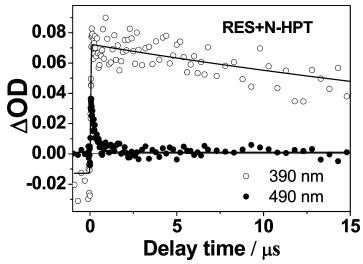

Figure 4. Time evolution profiles of N-HPT (1.5×10^{-3} M) and resveratrol (RES, 10×10^{-3} M) probed at 390 and 490 nm in acetonitrile following 355 nm photoexcitation (E_{exc} = 3 mJ/pulse) under anaerobic condition.

species absorbing at 390 nm decays (τ = 44 ± 3 μs), whereas this species is not seen to decay for acetonitrile solutions of N-HPT without resveratrol present.[14] The slowly decaying species is ascribed to the resveratrol radical generation from the reaction of resveratrol with the reactive radicals formed from homolytic cleavage of N-HPT, which will be further discussed below. The decay of the resveratrol radical in the mixture of N-HPT and resveratrol as monitored at 490 nm is fully described by a single exponential corresponding to a lifetime of 0.27 ± 0.01 μs slightly smaller than the lifetime found for the 490 nm kinetics for N-HPT alone (0.30 ± 0.01 μs). The reaction of $PyS^{\bullet}$ with resveratrol is accordingly seen to accelerate the decay of $PyS^{\bullet}$ under these conditions.

(3). Reaction of Resveratrol with Excited N-HPT in the Presence of Radical Scavengers. In order to clarify which of the possible reactive species are reacting with resveratrol, the radical scavenger MMA, scavenging both sulfur and hydroxyl radicals, and the radical scavenger *t*-BuOH, only scavenging hydroxyl radicals, were both used in competition experiments.[14,21,22] Transient absorption spectra following flash photolysis of resveratrol (1.0×10^{-2} M) mixed with N-HPT (1.5×10^{-3} M) recorded at 50 ns, 100 ns, and 5 μs in the absence and in the presence of *t*-BuOH (2.0 M) or MMA (2.0 M) in anaerobic acetonitrile are presented in Figure 5a−c. The transient spectra at a series of delay times in Figure 5a−c indicate that both *t*-BuOH and MMA reduce the intensity of transient spectra within the actual spectral region and actual time scale due to their scavenging of $PyS^{\bullet}$ or $^{\bullet}OH$. MMA was found more efficient in reducing the transient spectra intensity than *t*-BuOH. The long-lived species at 370−450 nm observed in the presence of MMA as seen in Figure 5c is suggested to be the resveratrol radical produced from direct photoexcitation. The spectral contribution from PySSPy is excluded on account

dx.doi.org/10.1021/jp3033337 | J. Phys. Chem. B 2012, 116, 7154−7161

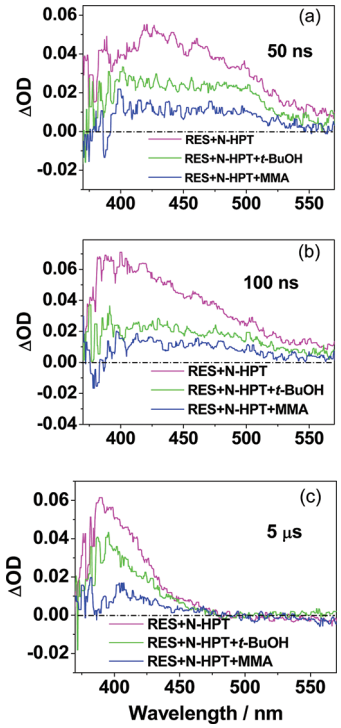

Figure 5. Transient absorption spectra at indicated delay time 50 ns (a), 100 ns (b), and 5 μs (c) of resveratrol (RES, 1.0×10^{-2} M) mixed with N-HPT (1.5×10^{-3} M) in the absence (red line) and in the presence of *t*-BuOH (2.0 M) (green line) or MMA (2.0 M) (blue line) in anaerobic acetonitrile. Excitation pulse energy was 3 mJ/pulse.

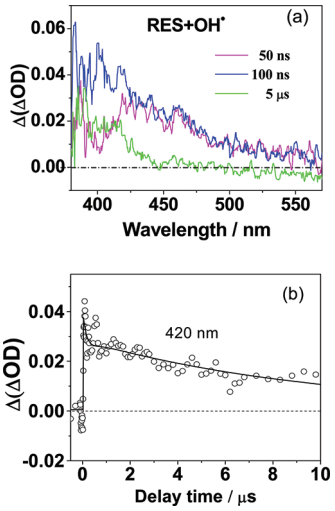

Figure 6. Time-associated difference spectra (a) and corresponding difference time evolutions (b) between absorption in the absence and in the presence of *t*-BuOH (2.0 M) corresponding to the radical of resveratrol formed by oxidation of resveratrol by the hydroxyl radical •OH in anaerobic acetonitrile.

of the fact that there is no long-lived PySSPy species observed at longer delay time when only NHPT is present in the photolyzed solution in the presence of MMA (cf. Figure S2 in the Supporting Information).

Under the actual conditions, *t*-BuOH was found to have no effect on the transient spectra of N-HPT following 355 nm laser photoexcitation (cf. Figure S3 in the Supporting Information). Compared with the transient spectra in the absence of *t*-BuOH, the reduction in the intensity of transient absorption in the presence of *t*-BuOH as seen in Figure 5a–c, is accordingly concluded to correspond to the absorption of the radicals of resveratrol formed from the reaction of resveratrol with •OH.

Difference spectra for photolysis of the mixed solution of resveratrol and N-HPT between in the absence and in the presence of *t*-BuOH (2.0 M) at the indicated delay times (50 ns, 100 ns, and 5 μs) are shown in Figure 6a. It may further be seen that resveratrol initially produces a short-lived species with a maximum at 420 nm as seen in the spectrum at 50 ns, which tends to transform into the other species at shorter wavelength appearing at 100 ns with an absorption maximum at ~390 nm. The former short-lived species is assigned as an adduct radical formed from •OH addition to resveratrol, and its nature will be further discussed below. The latter species is ascribed to the resveratrol 4′-phenoxyl radical due to the spectral similarity with the long-lived radical generated from direct photodissociation of resveratrol as seen in Figure 2a. The resveratrol 4′-phenoxyl radical is seen to be more stable than the initially formed resveratrol hydroxyl radical adduct. A comparison with the spectra of the product radical formed by the similar reaction of pterostilbene (3,5-methyl-*trans*-reveratrol) also confirms this assignment as shown in Figure S4 in the Supporting Information.

Figure 6b shows the time evolution for the *difference* in absorption of resveratrol and N-HPT at 420 nm in the absence and presence of *t*-BuOH following photolysis. This spectral difference corresponds to the resveratrol radical formed from the reaction of resveratrol with •OH. This time trace at 420 nm could be described by three exponentials as seen in Table 1 in agreement with a reaction sequence in which the initially formed resveratrol adduct radical decays with a time constant 0.21 ± 0.01 μs, and the 4′-phenoxyl radical appears as the other species with the same time constant 0.21 ± 0.01 μs and eventually decays with a slower rate with a time constant of 9.9 ± 0.9 μs. The good correlation seen for the decay of the adduct radical with the formation of 4′-phenoxyl radical strongly supports the transformation from the adduct radical into 4′-phenoxyl radical.

Table 1. Formation (f) and Decay (d) Time Constants Derived from Exponential Fitting of Kinetics Traces in Figures 6b and 7b

	420 nm		483 nm
τ_1	0.21 ± 0.01 μs (d)	τ	0.28 ± 0.04 μs (d)
τ_2	0.21 ± 0.01 μs (f)		
τ_3	9.9 ± 0.9 μs (d)		

The other radical scavenger, MMA, reported to scavenge both •OH and PyS•, accordingly restrains the formation of PySSPy. The *difference spectra* at 50 ns, 100 ns, and 5 μs, as shown in Figure 7a, between resveratrol and N-HPT photolyzed in the presence of *t*-BuOH and in the presence of MMA are further calibrated by subtracting the difference spectra at 5 μs in order to eliminate the spectral contributions from the long-lived PySSPy. The difference spectra in Figure 7a, after applying the second calibration, are found to have an absorption maximum ~483 nm, which may be assigned to the product of resveratrol reaction with the radical PyS•. The product is assigned as a radical adduct [RES···PyS]• formed by

dx.doi.org/10.1021/jp3033337 | J. Phys. Chem. B 2012, 116, 7154–7161

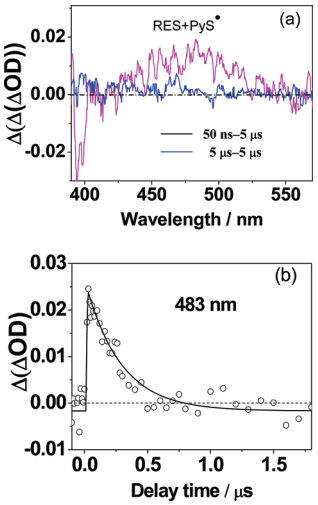

Figure 7. Time-associated difference spectra (a) between the difference spectra at 50 ns/100 ns/5 μs in the absence and in the presence of MMA (2.0 M) and the difference spectra at 5 μs corresponding to the radical of resveratrol (RES) formed by reaction between resveratrol and PyS$^\bullet$ and the corresponding difference time evolution (b) between absorption in the presence of *t*-BuOH (2.0 M) and absorption in the presence of MMA (2.0 M) in anaerobic acetonitrile. Time-associated difference spectra and time evolutions are calculated according to the relation: $(\Delta OD_{t\text{-BuOH}} - \Delta OD_{MMA})_{50/100ns/5\mu s} - (\Delta OD_{t\text{-BuOH}} - \Delta OD_{MMA})_{5\mu s}$, in which $\Delta OD_{t\text{-BuOH}}$ and ΔOD_{MMA} represent ΔOD in the presence of *t*-BuOH and MMA, respectively.

PyS$^\bullet$ addition to resveratrol.[23−25] The time evolution of absorption following photolysis of resveratrol and N-HPT at 483 nm is in Figure 7b seen as the difference between absorption recorded in the presence of *t*-BuOH and absorption recorded in the presence of MMA. The absorption decay at 483 nm could be described by a single exponential as seen in Table 1 with a time constant for the [RES···PyS]$^\bullet$ adduct radical of τ = 0.28 ± 0.04 μs. This adduct product of the thiyl radical addition to resveratrol is shown not to rearrange but seems rather stable.

Quantum Mechanical Calculations. Calculations were performed at the M06/6-31G* level of theory to determine the absolute energetics of the reactant complex (RS), transition states (TS), and product complex (PC) for the hydrogen atom transfer (HAT) and radical adduct formation (RAF) reactions of resveratrol with $^\bullet$OH as well as the absolute energetics of PC for electron transfer (ET) pathway. The results of these calculations are summarized in Table 2. Calculated absorption spectra of possible product radicals of resveratrol formed from oxidation of resveratrol by $^\bullet$OH are presented in Figure 8.

It is apparent from the results of the calculations presented in Table 2 that the reaction pathways of $^\bullet$OH addition to C2 or C6 of resveratrol have the lower energy of the transition states than those of other sites and thus are the most favorable pathway among the possible RAF and HAT reaction pathways. Table 2 is based on absolute energies presented for transition states and products. The ET pathway can be excluded due to the highest energetics of PC. Calculated absorption spectra of the product radicals formed from $^\bullet$OH addition to C2 or C6 of resveratrol are shown with a maximum at 442 or 422 nm as seen in Figure 8. The spectral position agrees well with the transient species experimentally observed at 50 ns as seen in Figure 6a, indicating that the most favorable pathway with respect to free energy is also found experimentally to be the faster one.

Table 2. Calculated Absolute Energies (hartrees) of the Transition States (TS) and the Product Radical (PR) and Absorption Wavelengths of PR in Acetonitrile at the M06-2X/6-31G* Level for Resveratrol (RES) Reaction with $^\bullet$OH by Hydrogen Atom Transfer (HAT), Radical Adduct Formation (RAF), and Electron Transfer (ET)

reaction mechanism	site	λ/nm	*E*/hartrees (TS)	*E*/hartrees (PR)
RES + $^\bullet$OH → RES(−H)$^\bullet$ + H_2O; HAT	3-OH	291	−841.742195	−841.798969
	5-OH	289	−841.742079	−841.798969
	4′−OH	366	−841.744103	**-841.809244**
RES + $^\bullet$OH → [RES···OH]$^\bullet$; RAF	C1′	243	−841.741600	−841.774453
	C2′	370	−841.747129	−841.787566
	C3′	273	−841.748366	−841.782417
	C4′	348	−841.744457	−841.790332
	C5′	270	−841.744744	−841.779201
	C6′	385	−841.745046	−841.782198
	C1	252	−841.737469	−841.767700
	C2	442	**-841.753336**	−841.792136
	C3	278	−841.741310	−841.777381
	C4	366	−841.750743	−841.794825
	C5	279	−841.741187	−841.774973
	C6	422	**-841.753259**	−841.793073
	C7	275	−841.752475	−841.806483
	C8	246	−841.750786	−841.806654
RES + $^\bullet$OH → RES$^{\bullet+}$···OH^-; ET	—	—	—	−841.6686852

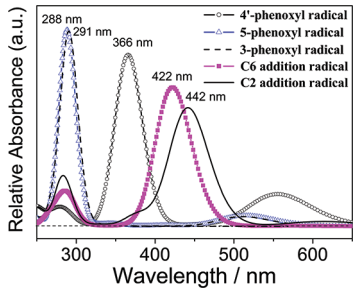

Figure 8. Calculated absorption spectra of the 3-, 5-, and 4′-phenoxyresveratrol radicals having maximum at 288, 291, and 366 nm, respectively, as formed by hydrogen atom transfer (HAT), and of the C2 and C6 hydroxyresveratrol having maximum at 442 and 422 nm as formed by radical adduct formation (RAF).

The comparisons for the absolute energy of resveratrol radicals at all possible reaction sites formed from the reaction of resveratrol with $^\bullet$OH radical in Table 2 demonstrate that the resveratrol 4′-phenoxyl radical is the most stable species, which is in agreement with the stability sequence of the two resveratrol radicals observed as shown in Figure 6a. The short-lived C2/C6 adduct radical (427 nm) tends to transform into the more stable 4′-phenoxyl radical (∼390 nm). The calculated absorption spectrum maximum for resveratrol 4′-phenoxyl radical differs by ∼20 nm (blue-shifted) relative to the experimentally observed spectra by laser photolysis, a difference which is considered acceptable provided the uncertainty in both the theoretical calculations and the transient absorption spectroscopy. Clearly, the long-lived radical of resveratrol is

dx.doi.org/10.1021/jp3033337 | J. Phys. Chem. B 2012, 116, 7154−7161

Scheme 2. Reactions of Resveratrol with Hydroxyl Radical and Thiyl Radical Generated from Homolytic Cleavage of N-HPT

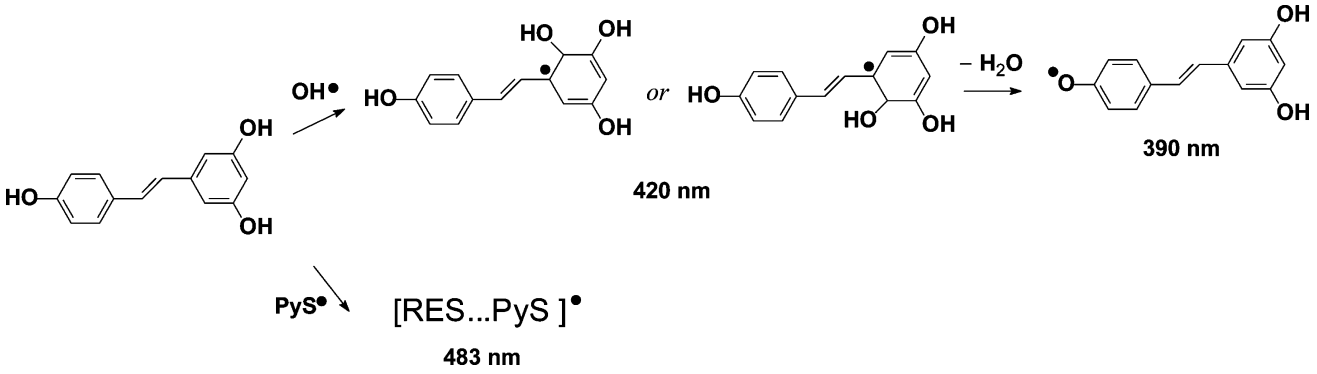

not the 3- or the 5-phenoxyl radical, which were calculated to have an absorption maximum at 288 and 291 nm, respectively. The weaker absorption bands shown in Figure 8 for each of the three phenoxyl radicals from the DFT calculations were not considered further in relation to the experimental work.

4. DISCUSSION

Resveratrol is known as an efficient radical scavenger and, since it is water-soluble, scavenging of radicals originating in the aqueous phase may be important for the beneficial health effects of resveratrol. Oxidative stress is under many conditions related to an excessive production of the superoxide radical anion or hydrogen peroxide in aqueous compartments of biological systems from which radicals attack membranes resulting in oxidative damage to unsaturated membrane lipids.[26] The superoxide radical anion dismutates spontaneously or enzymatically to hydrogen peroxide (and oxygen). Transition metals like copper and iron may readily react with hydrogen peroxide and further generate the hydroxyl radical being the most aggressive radical of biological relevance in what is known as the Fenton reaction:

$$2H^+ + 2O_2^{\bullet -} \rightarrow H_2O_2 + O_2 \quad (2)$$

$$H_2O_2 + Fe^{2+} \rightarrow {}^{\bullet}OH + OH^- + Fe^{3+} \quad (3)$$

Fe(II) may re-form from Fe(III) through reaction with reductants like ascorbate or even superoxide, establishing a catalytic cycle continually generating hydroxyl radicals. Hydroxyl radicals react with most organic molecules often in diffusion-controlled reactions and accordingly with little selectivity.[14] Antioxidants protecting cell structures should accordingly be located near the source of hydroxyl radical production. In the present study, the "photo-Fenton" reagent generated the hydroxyl radical, and resveratrol was shown to scavenge the hydroxyl radical efficiently. An important observation was that the initial product of hydroxyl radical scavenging by resveratrol was an unstable radical adduct (RAF mechanism) slowly converting into a more stable phenoxyl radical; see Scheme 2. The observation of a radical adduct excludes the possibilities of electron transfer and hydrogen atom transfer as the mechanism of the initial step in the reaction between the hydroxyl radical and resveratrol. Theoretical calculations (DFT) indicated that the transition state leading to the 2-hydroxyl resveratrol radical as product was of lower energy than the transition states leading to any other possible hydroxyl radical adducts of resveratrol through radical adduct formation (RAF mechanism) or leading directly to any of the three possible phenoxyl radicals through hydrogen atom transfer (HAT mechanism). Notably, only one radical adduct or a mixture of closely related adducts is being formed out of the many possible, indicating that the activation energy strictly controls the product distribution; i.e., the product distribution is kinetically controlled. Other factors of importance for the product distribution should, however, also be considered provided the fast reactions of the hydroxyl radical. The specific formation of one adduct, the 2-hydroxyresveratrol radical, maybe in a mixture with the 6-hydroxyresveratrol, could indicate some interaction between resveratrol and the hydroxyl generating reagent, N-HPT, such as hydrogen bonding of the singlet state of N-HPT to the resorcinol ring of resveratrol in an exiplex. Notably, the energy of the transition state for hydroxyl radical addition to C6 is only marginally larger than for C2. The difference could be caused by some steric hindrance from the rigid *trans*-ethylene brigde along the trajectory of the hydroxyl radical approaching C6. However, a mixture of C2 and C6 hydroxyl adducts may be formed as the primary product of the reaction of resveratrol with hydroxyl radical as seen in eq 4:

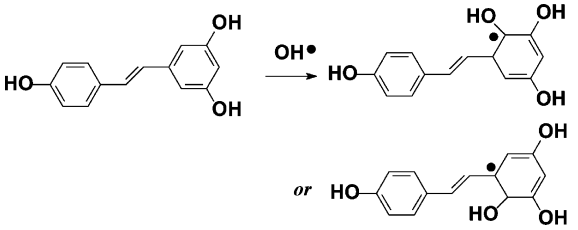

(4)

The initial product formed by addition of the hydroxyl radical to resveratrol is not the most stable as indicated by DFT calculations. Any of the three phenoxyl radicals of resveratrol has lower energy than the adduct radicals, and the hydroxyl radical adduct of resveratrol converts in a process with a rate constant of 5×10^6 s^{-1} to the 4′-phenoxyresveratrol as the most stable phenoxyl radical (see Table 1). The rate is comparable to the rate constant (4×10^5 s^{-1}) determined for a similar radical delocalization process for radicals formed from photooxidation of isoflavonones.[27] In the conversion of the hydroxyresveratrol to the 4′-phenoxyresveratrol, a water molecule is lost and this process could be triggered by the increased acidity of the hydroxyl resveratrol radical as compared to resveratrol. The 4′-hydroxy group is the more acidic with pK_a = 6.4 in aqueous solution,[10] a value which will decrease upon radical formation leading to an intramolecular proton transfer generating H_2O as a good leaving group at C2 or C6, further leading to the following proposed sequency of reactions:

dx.doi.org/10.1021/jp3033337 | J. Phys. Chem. B 2012, 116, 7154–7161

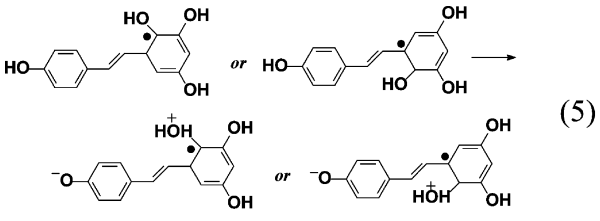

(5)

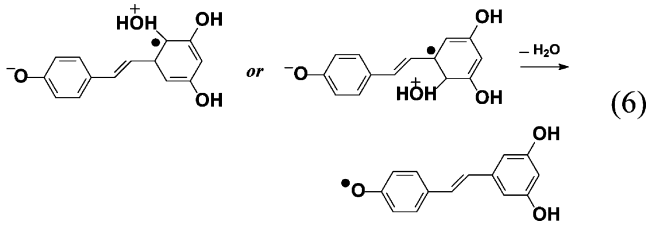

(6)

In reaction 4, the 2- or 6-hydroxy radical adduct of resveratrol is formed, which subsequently transfers a proton in a fast reaction 5 leading to the reactant, which upon dissociation of a water molecule and concomintant rearrangement forms the 4′-phenoxyresveratrol radical in a rate-determining reaction 6. The 4′-phenoxyresveratrol radical is relatively stable but decays slowly probably through disproportionation or dimerization reactions. The conversion of the 2- or 6-hydroxyresveratrol radical adduct to the 4′-phenoxyresveratrol radical through the reactions of eqs 5 and 6 involves a stepwise proton-assisted electron transfer. Alternatively, a hydrogen atom could be transferred directly (HAT) as shown in the reaction of eq 7:

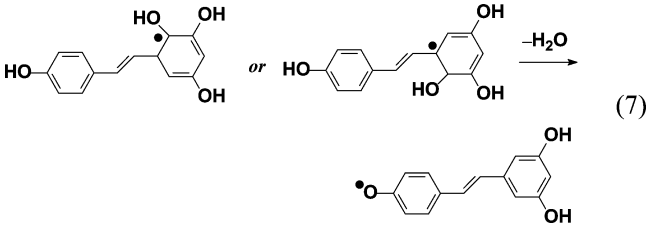

(7)

Hydrogen atom transfer is expected to occur slower than the stepwise proton-assisted electron transfer, and the moderately high rate constant of 5×10^6 s^{-1} could be in favor of the HAT mechanism.[28−30]

This study shows that resveratrol reacts efficiently with both oxygen-centered and sulfur-centered radicals. The hydroxyl radical is a oxygen-centered radical with little specificity. Probably the most important finding is that •OH forms only one or two colosely related initial products with resveratrol, and that the dominating addition product is the addition product for which the reaction path encounters the lowest energy of activation, and not the more stable product, to which rearrangement subsequently is occurring. In contrast to this kinetically controlled product distribution, the thiyl radical forms the most stable radical addition product without any detectable intermediates.

Resveratrol is an effective scavenger of hydroxyl radicals through an addition reaction. It should, however, be noted that other factors also influence the effectiveness of polyphenols as antioxidants as measured by more practical oriented methods like the ORAC assay (oxygen absorbance capacity) and assays based on scavenging of semistable radicals like the galvinoxyl radical.[35] Often a catechol moiety is found crucial for an effective polyphenol antioxidant in such assays due to radical stabilization by resonance.

■ ASSOCIATED CONTENT

Supporting Information

Transient absorption spectra under aerobic conditions of resveratrol, transient absorption spectra of N-HPT, molecular structures and time-associated difference spectra of pterostilbene, and complete ref 15. This material is available free of charge via the Internet at http://pubs.acs.org.

■ AUTHOR INFORMATION

Corresponding Author

*Tel: +86-10-6251-6604 (R.-M.H.); +45-3528-3221 (L.H.S.). Fax: +86-10-6251-6444 (R.-M.H.); +45-3528-3344 (L.H.S.). E-mail: rmhan@chem.ruc.edu.cn (R.-M.H.); ls@life.ku.dk (L.H.S.).

Notes

The authors declare no competing financial interest.

■ ACKNOWLEDGMENTS

This work has been supported by the Natural Science Foundation of China (20803091, 20933010) and the Fundamental Research Funds for the Central Universities (RUC No. 10XNI007). L.H.S. thanks the Danish Research Council for Independent Research, Technology and Production Science for continuing support currently as the grant 09-065906/FTP: Redox Communication in the digestive tract.

■ REFERENCES

(1) Fabris, S.; Momo, F.; Ravagnan, G.; Stevanato, R. *Biophys. Chem.* **2008**, *135*, 76−83.
(2) Jang, M; Cai, L; Udeani, G. O.; Slowing, K. V.; Thomas, C. F.; Beecher, C. W.; Fong, H. H.; Farnsworth, N. R.; Kinghorn, A. D.; Mehta, R. G.; Moon, R. C.; Pezzuto, J. M. *Science* **1997**, *275*, 218−220.
(3) Constant, J. *Coronary Artery Dis.* **1997**, *8*, 645−649.
(4) Fremont, L. *Life Sci.* **2000**, *66*, 663−673.
(5) Frankel, E. N.; Waterhouse, A. L.; Kinsella, J. E. *Lancet* **1993**, *341*, 1103−1104.
(6) Gutteridge, J. M. C. *Free Radical Res. Commun.* **1993**, *19*, 141−158.
(7) Halliwell, B.; Gutteridge, J. M. C. *Lancet* **1984**, *1*, 1396−1398.
(8) Halliwell, B.; Gutteridge, J. M. C. *Lancet* **1984**, *2*, 1095−1095.
(9) Shang, Y.-J.; Qian, Y.-P.; Liu, X.-D.; Dai, F.; Shang, X.-L.; Jia, W.-Q.; Liu, Q.; Fang, J.-G.; Zhou, B. *J. Org. Chem.* **2009**, *74*, 5025−5031.
(10) Stojanović, S.; Brede, O. *Phys. Chem. Chem. Phys.* **2002**, *4*, 757−764.
(11) Bader, Y.; Quint, R. M.; Getoff, N. *Radiat. Phys. Chem.* **2008**, *77*, 708−712.
(12) Helmut, S. *Eur. J. Biochem.* **1993**, *215*, 213−219.
(13) Wouters, M. A.; Fan, S. W.; Haworth, N. L. *Antioxid. Redox Signal* **2010**, *12*, 53−91.
(14) Chen, C.-H.; Han, R.-M.; Liang, R.; Fu, L.-M.; Wang, P.; Ai, X.-C.; Zhang, J.-P.; Skibsted, L. H. *J. Phys. Chem. B* **2011**, *115*, 2082−2094.
(15) Frisch, M. J.; Trucks, G. W.; Schlegel, H. B.; Scuseria, G. E.; Robb, M. A.; Cheeseman, J. R.; Scalmani, G.; Barone, V.; Mennucci, B.; Petersson, G. A.; et al. *Gaussian 09, Revision A.02*; Gaussian, Inc.: Wallingford, CT, 2009.
(16) Tomasi, J.; Mennucci, B.; Cancès, E. *J. Mol. Struct. (THEOCHEM)* **1999**, *464*, 211−226.
(17) Gorelsky, S. I. Swizard program, http://www.sg-chem.net/; University of Ottawa: Ottawa, Canada, 2010.
(18) Petralia, S.; Spatafora, C.; Tringali, C.; Foti, M. C.; Sortino, S. *New J. Chem.* **2004**, *28*, 1484−1487.

(19) Stojanović, S.; Sprinz, H.; Brede, O. *Arch. Biochem. Biophys.* **2001**, *391*, 79−89.
(20) DeMatteo, M. P.; Poole, J. S.; Shi, X.; Sachdeva, R.; Hatcher, P. G.; Hadad, C. M.; Platz, M. S. *J. Am. Chem. Soc.* **2005**, *127*, 7094−7109.
(21) Ito, O.; Matsuda, M. *J. Am. Chem. Soc.* **1979**, *101*, 5732−5735.
(22) Ito, O.; Matsuda, M. *J. Am. Chem. Soc.* **1981**, *103*, 5871−5874.
(23) Hung, W.-L.; Ho, C.-T.; Hwang, L. S. *J. Agric. Food. Chem.* **2011**, *59*, 1968−1973.
(24) Goldstein, S.; Samuni, A.; Merenyi, G. *J. Phys. Chem. A* **2008**, *112*, 8600−8605.
(25) El.-Agamey, A.; Fukuzumi, S.; Naqvi, K. R.; McGarvey, D. J. *Org. Biomol. Chem.* **2011**, *9*, 1459−1465.
(26) Skibsted, L. H. Understanding oxidation processes in foods. In *Oxididation in foods and beverages and antioxidant applications*; Decker, E. A., Elias, R. J., McClements, D. J., Eds.; Woodhead Publishing: Cambridge, UK, 2010.
(27) Tian, Y.-X.; Han, R.-M.; Fu, L.-M.; Zhang, J.-P.; Skibsted, L. H. *J. Phys. Chem. B* **2008**, *112*, 2273−2280.
(28) Warren, J. J.; Tronic, T.; Mayer, J. M. *Chem. Rev.* **2010**, *110*, 6961−7001.
(29) Litwinienko, G.; Ingold, K. U. *Acc. Chem. Res.* **2007**, *40*, 222−230.
(30) Cardoso, D. R.; Libardi, S. H.; Skibsted, L. H. *Food Funct.* **2012**, *3*, 487−502.
(31) Gadosy, T. A.; Shukla, D.; Johnston, L. J. *J. Phys. Chem. A* **1999**, *103*, 8834−8839.
(32) Corduneanu, O.; Janeiro, P.; Oliveira Brett, A. M. *Electroanalysis* **2006**, *18*, 757−762.
(33) Brittes, J.; Lúcio, M.; Nunes, C.; Lima, J. L.; Reis, S. *Chem. Phys. Lipid* **2010**, *163*, 747−754.
(34) Xu, S.; Wang, G.; Liu, H.-M.; Wang, L.-J.; Wang, H.-F. *J. Mol. Struct. (THEOCHEM)* **2007**, *809*, 79−85.
(35) Yilmaz, Y.; Toledo, R. T. *J. Agric. Food Chem.* **2004**, *52*, 255−260.